The Inland Maintenance and Reintensification of Tropical Storm Bill (2015). Part I: Contributions of the Brown Ocean Effect

RYANN A. WAKEFIELD,[a] JEFFREY B. BASARA,[a,b] J. MARSHALL SHEPHERD,[c] NOAH BRAUER,[a] JASON C. FURTADO,[a] JOSEPH A. SANTANELLO JR.,[d] AND ROGER EDWARDS[e]

[a] *School of Meteorology, University of Oklahoma, Norman, Oklahoma*
[b] *School of Civil Engineering and Environmental Science, University of Oklahoma, Norman, Oklahoma*
[c] *Program in Atmospheric Sciences, Department of Geography, University of Georgia, Athens, Georgia*
[d] *Hydrological Sciences Branch, NASA Goddard Space Flight Center, Greenbelt, Maryland*
[e] *NWS Storm Prediction Center, Norman, Oklahoma*

(Manuscript received 19 June 2020, in final form 2 July 2021)

ABSTRACT: Landfalling tropical cyclones (TCs) often decay rapidly due to a decrease in moisture and energy fluxes over land when compared to the ocean surface. Occasionally, however, these cyclones maintain intensity or reintensify over land. Post-landfall maintenance and intensification of TCs over land may be a result of fluxes of moisture and energy derived from anomalously wet soils. These soils act similarly to a warm sea surface, in a phenomenon coined the ''brown ocean effect.'' Tropical Storm (TS) Bill (2015) made landfall over a region previously moistened by anomalously heavy rainfall and displayed periods of reintensification and maintenance over land. This study evaluates the role of the brown ocean effect on the observed maintenance and intensification of TS Bill using a combination of existing and novel approaches, including the evaluation of precursor conditions at varying temporal scales and making use of composite backward trajectories. Comparisons were made to landfalling TCs with similar paths that did not undergo TC maintenance and/or intensification (TCMI) as well as to TS Erin (2007), a known TCMI case. We show that the antecedent environment prior to TS Bill was similar to other known TCMI cases, but drastically different from the non-TCMI cases analyzed in this study. Furthermore, we show that contributions of evapotranspiration to the overall water vapor budget were nonnegligible prior to TCMI cases and that evapotranspiration along storm inflow was significantly ($p < 0.05$) greater for TCMI cases than non-TCMI cases suggesting a potential upstream contribution from the land surface.

KEYWORDS: Evapotranspiration; Feedback; Hurricanes/typhoons; Mesoscale processes; Surface fluxes; Water vapor

1. Introduction and background

Soil moisture can play a role in the development of weather and climate extremes, particularly within continental regions comprised of a transition zone from humid to drier climates such as the southern Great Plains (Guo et al. 2006; Koster et al. 2004, 2006; Dirmeyer 2006). In these regions a greater sensitivity of the overlying atmosphere to surface fluxes is observed, in some cases, reinforcing precipitation anomalies via soil moisture memory (Koster and Suarez 2001) and influence on large-scale dynamics (Namias 1988). In other cases, surface fluxes may be sufficient in magnitude and partitioning to disrupt precipitation anomalies (Wu and Dirmeyer 2020) as is the case when large sensible heat fluxes trigger convection over dry soils (Findell and Eltahir 2003; Tawfik and Dirmeyer 2014; Taylor et al. 2012; Ford et al. 2015). The sign of these feedbacks is largely dependent upon the spatial and temporal scales being considered (Guillod et al. 2015). Changes to land use and land cover can also impact precipitation extremes. This is evident even in arid regions where afforestation can provide localized rainfall enhancement (Yosef et al. 2018; Branch and Wulfmeyer 2019). Elsewhere, anthropogenic land use changes have been linked to reductions in precipitation a result of increased irrigation and agricultural use in the Indian monsoon region (Niyogi et al. 2010). Thus, the land surface can even impact larger-scale atmospheric circulations. Antecedent positive rainfall anomalies have been associated with further inland penetration of landfalling monsoon depressions (Kishtawal et al. 2013) and has also been shown to increase their intensity (Chang et al. 2009). Dastoor and Krishnamurti (1991) showed that more accurate parameterization of soil wetness produced more accurate simulations of rainfall associated with landfalling tropical cyclones over India. Landfalling tropical cyclones may be similarly impacted by soil wetness and other land surface characteristics. Tropical cyclones (TC) are fueled by fluxes of heat and moisture from the surface, in particular, a warm sea surface (e.g., Emanuel et al. 2004). Reduction in evaporation upon landfall contributes to tropical cyclone decay over land (Tuleya and Kurihara 1978; Tuleya 1994) though landfalling TCs may be sustained by fluxes of heat and moisture from the land surface even as they move away from oceanic basins. This phenomenon is referred to as the "brown ocean effect" (Andersen and Shepherd 2013), which broadly refers to instances when landfalling tropical cyclones maintain or reintensify over land as a result of positive soil moisture anomalies.

Wakefield's current affiliations: Cooperative Institute for Research in Environmental Sciences, University of Colorado, Boulder, and NOAA/Global Systems Laboratory, Boulder, Colorado.

Corresponding author: Ryann A. Wakefield, ryann.wakefield@noaa.gov

DOI: 10.1175/JHM-D-20-0150.1

© 2021 American Meteorological Society. For information regarding reuse of this content and general copyright information, consult the AMS Copyright Policy (www.ametsoc.org/PUBSReuseLicenses).

Brought to you by UNIVERSITY OF OKLAHOMA LIBRARY | Unauthenticated | Downloaded 10/13/21 07:32 PM UTC

Post-landfall intensification of TCs is typically a result of the storm interacting with a midlatitude baroclinic zone and transitioning to an extratropical cyclone (Hart and Evans 2001; Jones et al. 2003; Evans et al. 2011). Occasionally, overland reintensification may instead be attributed to sufficient fluxes of moisture and energy from wet soils, as stated by the brown ocean effect (Andersen and Shepherd 2013). Numerical simulations of landfalling TCs are sensitive to parameterizations of the land surface (Bozeman et al. 2011; Kishtawal et al. 2011). Simulated landfalling TCs (Shen et al. 2002) still weaken when moving over a water-covered land surface, but they do so more slowly than those over dry land. Moreover, these TCs display a much greater diurnal cycle in convection than TCs over the ocean due to lower heat capacity of a flooded landscape (Shen et al. 2002).

Emanuel et al. (2008) suggested that daytime heating and moistening of sandy soils from outer rainbands ahead of the path of landfalling TCs in Australia provide sufficient latent heat flux to fuel maintenance or intensification of the TC as it moves further inland. This theory was proposed to explain the inland reintensification of TS Erin over Oklahoma on 19 August 2007 (Emanuel et al. 2008; Kellner et al. 2012). Antecedent (March–July) rainfall in the region was well above normal (Arndt et al. 2009); however, in the weeks preceding Erin's landfall, top-level soil had dried and warmed markedly along the path such that outer rainbands ahead of Erin could remoisten soils and lead the way to enhanced interband latent heat flux (Arndt et al. 2009; Evans et al. 2011; Monteverdi and Edwards 2010; Andersen et al. 2013).

This brown ocean effect may play a role in the reintensification of TCs in North America, Asia, and Australia (Andersen and Shepherd 2013). Through a global climatology of inland TC maintenance and/or intensification (TCMI), Andersen and Shepherd (2013) found that latent heat fluxes were much greater in the vicinity of a TCMI during the 3 weeks prior to, as well as during, the TCMI occurrence when compared to TCs that weakened over land. In other words, antecedent *and* concurrent surface moisture both play a role in TCMI, via increased latent heat fluxes making it necessary to examine land surface conditions related to TCMI cases at multiple time scales. Furthermore, daytime maximum latent heat fluxes over land during the period preceding TCMI occurrences are often similar in magnitude to latent heat fluxes over the ocean (Andersen et al. 2013). More recently, Nair et al. (2019) found that an unnamed depression responsible for intense flooding in Louisiana may have been enhanced by the brown ocean effect.

Recently, in the United States, both TS Erin (2007) and TS Bill (2015) maintained warm-core characteristics for an extended period of time post-landfall. In both cases, above-normal antecedent precipitation had occurred along the paths of each storm. Previous studies have explored the potential drivers of Erin's reintensification over Oklahoma (Arndt et al. 2009; Monteverdi and Edwards 2010), but there is a dearth of literature regarding the post-landfall evolution of TS Bill. A series of Weather Prediction Center Tropical Advisory Discussions from 2100 UTC 19 June 2015 to 1500 UTC 20 June 2015 acknowledged the potential role that antecedent rainfall may have played in Bill's reintensification (Rubin-Oster 2015). However, Zhang et al. (2019) refute this claim, instead suggesting that increased soil moisture would contribute to the weakening of TS Bill post-landfall, through increased vertical mixing, and boundary layer stabilization. Within the storm environment, beyond the main circulation, diabatic heating effects enhanced vertical vorticity and convective instability supporting a more symmetric structure over land, and thus, maintenance of intensity in a simulated TS Bill (Zhang et al. 2020). Thus, it is important to consider the role of latent and sensible heat fluxes within the environment adjacent to the storm itself.

This study uses a novel application of existing and novel methods to evaluate the precursor environment along the path of TS Bill to determine whether prestorm environment was supportive of the inland maintenance and/or intensification of TS Bill. We hypothesize that anomalously moist soils supported the overland maintenance of TS Bill for more than four days following landfall through anomalous latent heat fluxes, both near the storm's center and along the trajectories of inflow parcels. The current study implements a multistep process for assessing whether anomalous moisture fluxes from the land surface provided an environment supportive of the overland maintenance and reintensification of Tropical Storm Bill. Sections 2 and 3 present an overview of TS Bill, the data analyzed and our TCMI classification criteria. Finally, we analyze the event using three different approaches, and we group each analysis with its results in sections 4, 5, and 6. First, we examine the evolution of surface moisture fluxes and atmospheric moisture during the 2-week period leading up to a potential TCMI event, building on metrics from Andersen and Shepherd (2013). We identify landfalling storms with a similar path that did not undergo TCMI and compare our results to our TCMI cases. Then, we focus on a shorter time scale and the relative contributions of evapotranspiration to the atmospheric water vapor budget during the 72-h period preceding TCMI and non-TCMI storms. The third and final part of the analysis evaluates 24-h accumulated evapotranspiration along the path of inflow parcels for each storm in the study. Discussion and conclusions of our results follow.

2. TS Bill (2015) overview

Table 1 summarizes the track of TS Bill. TS Bill became a named storm at 0000 UTC 16 June over the Gulf of Mexico and tracked northwestward before making landfall on Matagorda Island, Texas, at 1645 UTC. TS Bill's maximum intensity was observed shortly before and following landfall from 1200 to 1800 UTC 16 June, with a central pressure of 997 hPa and maximum sustained surface winds at 50 kt ($26\,m\,s^{-1}$; $1\,kt \approx 0.51\,m\,s^{-1}$). As Bill progressed northward through Texas, it weakened and was reclassified by the National Hurricane Center as a tropical depression at 0600 UTC on 17 June. Despite moving further inland, Bill maintained a central pressure of 999 hPa from 0600 to 1800 UTC 17 June, though maximum sustained winds decreased from 30 to 25 kt during the same period. Following this period of relatively constant

Brought to you by UNIVERSITY OF OKLAHOMA LIBRARY | Unauthenticated | Downloaded 10/13/21 07:32 PM UTC

TABLE 1. Summary of NHC best track data for Tropical Storm Bill (2015). TCMI events are highlighted in bold.

Date/time (UTC)	Pressure (hPa)	Wind speed (kt)	Category	Date/time (UTC)	Pressure (hPa)	Wind speed (kt)	Category
16/0000	1005	45	TS	18/1200	1003	15	TD
16/0600	1001	45	TS	18/1800	1004	15	Low
16/1200	997	50	TS	19/0000	1005	15	Low
16/1645	997	50	TS	19/0600	1006	15	Low
16/1800	997	50	TS	**19/1200**	**1006**	**15**	**Low (TCMI2)**
17/0000	998	40	TS	**19/1800**	**1005**	**20**	**Low (TCMI2)**
17/0600	999	30	TD	**20/0000**	**1004**	**20**	**Low (TCMI2)**
17/1200	**999**	**30**	**TD (TCMI1)**	**20/0600**	**1002**	**15**	**Low (TCMI2)**
17/1800	**999**	**25**	**TD (TCMI1)**	**20/1200**	**1001**	**15**	**Low (TCMI2)**
18/0000	1000	25	TD	20/1800	1003	15	Low
18/0600	1002	20	TD	21/0000	1006	15	Low

intensity, Bill began to weaken and curved northeastward before being classified as a remnant low by 1800 UTC 18 June in eastern Oklahoma. Bill produced rainfall > 30 cm in some places (Berg 2015; Stewart 2016) along with 19 tornadoes resulting from its remnant circulation recorded in the Storm Prediction Center TC tornado data (TCTOR; Edwards 2010) as it tracked over land from 16 to 21 June. Between 1200 UTC 19 June and 1200 UTC 20 June, Bill's central pressure dropped from a mean sea level pressure (MSLP) of 1006 hPa to 1001 hPa as it moved from southern Missouri to northwestern Kentucky. Radar imagery of Bill during this time (not shown) indicated enhanced convective activity to the southeast and a defined cyclonic circulation. According to the Weather Prediction Center (WPC) public advisory archive (Rubin-Oster 2015), satellite imagery also displayed prominent upper-level outflow to the north.

Similar to 2007 when TS Erin reintensified over Oklahoma, 2015 was characterized by anomalously heavy rainfall preceding the arrival of TS Bill. Bill's period of reintensification on 19 and 20 June may have been supported by anomalously wet land surface conditions as upper-level forcing was minimal. Further, TS Bill also displayed a period of near-constant central pressure over northern Texas despite its inland location. As such, this study will also assess whether the prestorm environment is supportive of brown ocean effect in relation to the maintenance and intensification of TS Bill over land. The objective of this study is not to reassess the existence of the brown ocean effect, but rather to determine whether TS Bill exhibited similar characteristics to another landfalling tropical cyclone which maintained intensity or reintensified over land.

3. Data

a. HURDAT2

National Hurricane Center Best Track data, for TS Bill and the other three storms analyzed, were obtained from the publicly available HURDAT2 database (Landsea and Franklin 2013) which contains information about Atlantic basin tropical cyclones which occurred between 1851 and 2019. Latitude, longitude, central sea level pressure, and 1-min maximum sustained surface wind speed (10 m AGL) are provided at 6-hourly intervals, as well as information about the cyclone's classification, landfall, and maximum intensity.

b. North American Regional Reanalysis

Meteorological surface and pressure level variables (Table 2) were obtained from the 3-hourly North American Regional Reanalysis (NARR) dataset (Mesinger et al. 2006). The NARR assimilates satellite and in situ observations of pressure level and surface meteorological quantities including temperature, moisture as well as precipitation gauge data, into the National Centers for Environmental Prediction (NCEP) Eta Model to produce a 3-hourly gridded dataset with 32-km resolution and 29 vertical pressure levels. Vertical levels are distributed nonuniformly from 1000 to 10 hPa on a Northern Hemisphere Lambert Conformal Conic Grid. Further, the ability of the NARR to represent land–atmosphere coupling processes (Santanello et al. 2015) and its past applications toward similar studies (Kellner et al. 2012) make it an appropriate choice to assess the impact of land surface fluxes on inland TCs. Latent heat flux, total column precipitable water (PWAT) and total-column water vapor convergence (WVC) 3-hourly data were obtained for the 2-week periods preceding each time analyzed for each TC. For example, data were obtained for the 2-week period ending 0000 UTC 16 June 2015 as well as the 2-week period ending 0600 UTC 20 June 2015 as both dates were considered in the analysis of TS Bill. Because best track data are provided at 6-hourly intervals, we can match that data with appropriate corresponding NARR time, and the nearest 3-hourly time step to each time of interest along the storm's track. While landfall times were often between the 3-hourly NARR intervals, this discrepancy did not impact the analysis, as the focus of this study is on inland TCs and TCMI analyses were not focused on the storm at landfall.

4. TCMI classification

Classification of TCMI events was designed to be consistent with previous studies. Andersen and Shepherd (2013) established that a minimum distance of 350 km from a tropical

Brought to you by UNIVERSITY OF OKLAHOMA LIBRARY | Unauthenticated | Downloaded 10/13/21 07:32 PM UTC

TABLE 2. Summary of variables obtained from the North American Regional Reanalysis.

Variable	Description	Vertical level
Accumulated total precipitation (kg m^{-2})	3-hourly accumulation	Surface
Precipitable water for entire atmosphere (kg m^{-2})	3-hourly mean	Total atmospheric column
Latent heat flux (W m^{-2})	3-hourly mean (from forecast output)	Surface
Specific humidity (kg kg^{-1})	3-hourly mean	Surface and pressure level
Air temperature (K)	3-hourly mean	Surface and pressure level
Zonal wind (m s^{-1})	3-hourly mean	Pressure level
Meridional wind (m s^{-1})	3-hourly mean	Pressure level
Pressure level (hPa)	Constant levels	1000, 975, 950, 925, 900, 875, 850, 825, 800, 775, 750, 725, 700, 650, 600, 550, 500, 450, 400, 350, 300, 275, 250, 225, 200, 175, 150, 125, 100

cyclone (TC) center to the nearest oceanic moisture source is necessary to properly assess the relative influence of the land surface. This minimum distance ensures that the majority of the TC circulation, which typically occurs within a 4°–6° radius (Frank 1977), was over land at the time of analysis. Therefore, in this study, TCMI was evaluated along the TC path only when the TC was >350 km from the nearest ocean basin (Fig. 1).

Next, the TC must still display tropical characteristics at the time of inland intensification. These characteristics include temperature maxima near the core of the cyclone, vertical stacking of lows at successive height levels, and wind speed that decreases with height, consistent with the thermal wind relation (Monteverdi and Edwards 2010). Equivalent potential temperature (θ_e) was examined at 700 and 500 hPa to determine whether the core of TS Bill was warmer than the environment within a 6° radius. The companion analysis to this paper uses polarimetric radar variables to show that TS Bill continued to display warm rain signatures consistent with tropical cyclone precipitation characteristics (Brauer et al. 2021, hereafter Part II) during its track over land.

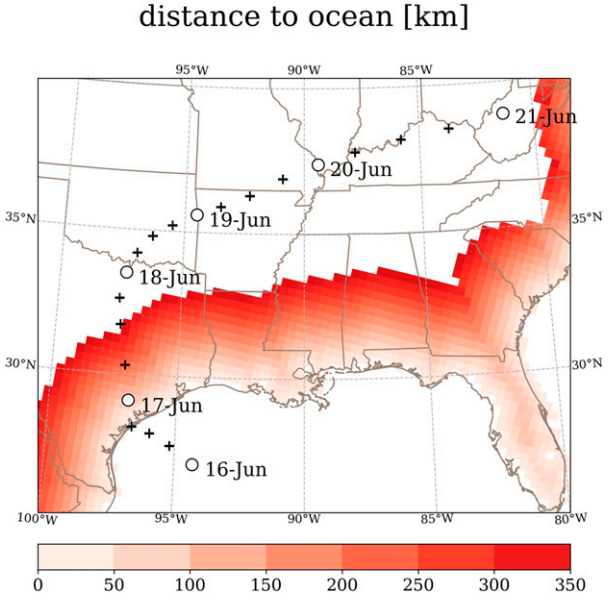

FIG. 1. Distance from nearest ocean basin (shaded up to 350 km) and Tropical Storm Bill (2015) track. White filled circles represent 0000 UTC location while plus signs represent location at 0600, 1200, and 1800 UTC.

A period of relatively consistent intensity occurred over much of Central Texas, during which time TS Bill produced excessive rainfall across portions of Texas, Louisiana and Oklahoma (Stewart 2016). TS Bill maintained a central pressure of 999 hPa over land from 17 June 0600 UTC through 17 June 1800 UTC, though only the period from 1200 to 1800 UTC met the >350-km oceanic-distance constraint of Andersen and Shepherd (2013). This period, from 1200 to 1800 UTC 17 June was defined as TCMI1 (Table 1). By 1200 UTC TS Bill was far enough from the Gulf of Mexico to be considered a TCMI event (Fig. 2); however, maximum sustained winds decreased from 30 to 25 kt (15–13 m s^{-1}), despite constant minimum central pressure. A second TCMI event, TCMI2, was defined by the period of decreasing central pressure observed from 1200 UTC on 19 June to 1200 UTC 20 June. We used pressure level temperature and specific humidity obtained from the NARR to compute equivalent potential temperature θ_e at 500 and 700 hPa. Area-averaged θ_e was computed for all points within 0.5° of the storm center at 500 and 700 hPa. We then computed the difference between equivalent potential temperature at all points within the NARR domain, but outside of the 0.5° radius (i.e., environmental θ_e) and the average within the 0.5° radius (i.e., TC center θ_e) during TCMI1, at 1800 UTC 17 June (Fig. 3) and during TCMI2, at 0600 UTC 20 June (Fig. 4). Thus, the color shown at each point is the difference between that point's θ_e and the mean θ_e within 0.5° of the storm center. This was performed for the sole purpose of demonstrating that θ_e was maximized near the center of TS Bill during each TCMI event, consistent with the storm retaining tropical characteristics. This was not the only method used to determine whether TS Bill retained its tropical characteristics over land. Details regarding the tropical precipitation characteristics of TS Bill over land can be found in Part II.

5. Two-week antecedent environment

To better understand atmospheric preconditioning in relation to persistent soil moisture anomalies, we analyzed surface

Brought to you by UNIVERSITY OF OKLAHOMA LIBRARY | Unauthenticated | Downloaded 10/13/21 07:32 PM UTC

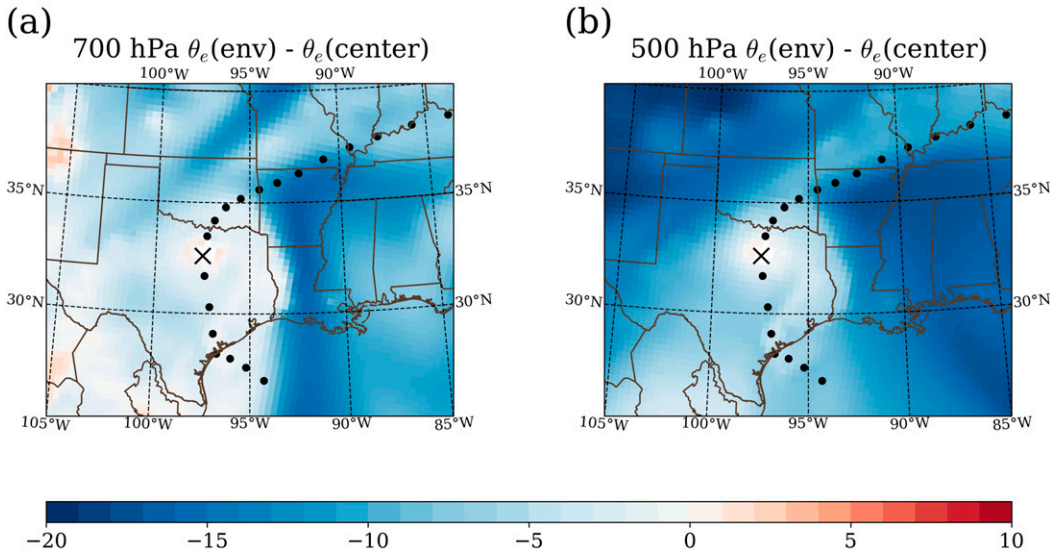

FIG. 2. Difference from 0.5° area-averaged equivalent potential at 1800 UTC 17 Jun 2015 at (a) 700 and (b) 500 hPa. Area-averaged equivalent potential temperature was obtained by averaging equivalent potential temperature within a 0.5° radius of the storm center on 1800 UTC 17 June, while the environment is defined as all points outside of this region. Blue means that the environment is cooler than the 0.5° average.

fluxes and precipitation during the antecedent 2-week period prior to each storm. We chose the 2-week time window to facilitate comparison between NARR fluxes during TS Bill and those of TCMI events considered in past studies. In particular, we were interested in how TCMI events during Bill compared with TS Erin (2007) analyzed in Andersen et al. (2013). The choice of a 2-week antecedent period was also motivated by soil moisture memory. In other words, changes in land surface moisture are slower than changes in atmospheric moisture. Consequently, excessive precipitation is ''remembered'' by the land surface and reflected in higher latent heat fluxes. A continuous supply of moisture via precipitation maintains a moist land surface that can then provide a continuous flux of moisture back into the atmosphere via evapotranspiration (ET). This constant supply ensures that the rate of evaporation is constrained only by the atmospheric demand, and therefore, sufficient net radiation. As soil moisture depletes over a period of weeks to months (Koster and Suarez 2001), the 2-week antecedent period provides an important understanding of how excessive precipitation during 2015 could be linked to Bill's

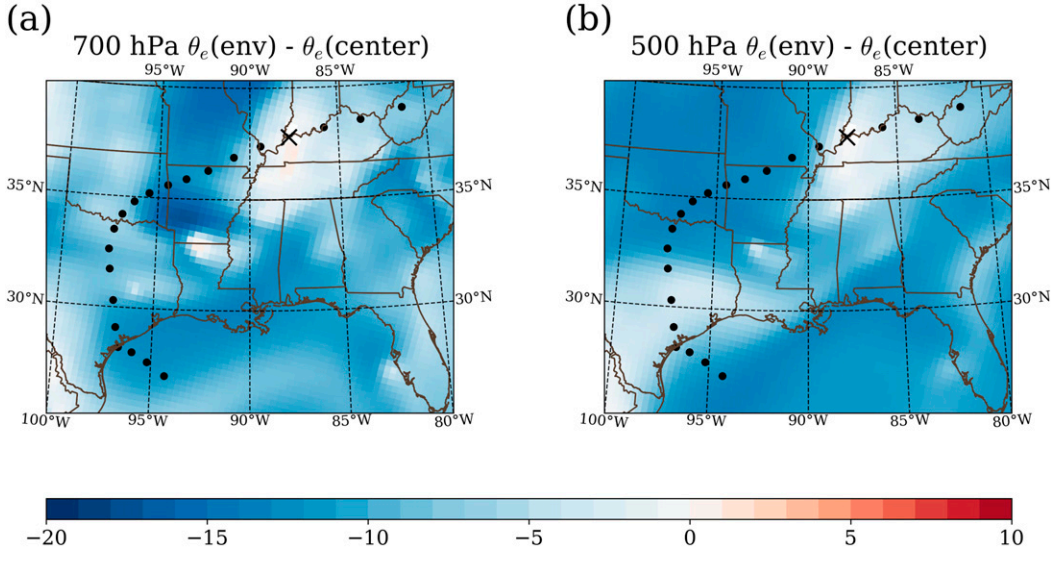

FIG. 3. As in Fig. 2, but at 0600 UTC 20 Jun 2015.

Brought to you by UNIVERSITY OF OKLAHOMA LIBRARY | Unauthenticated | Downloaded 10/13/21 07:32 PM UTC

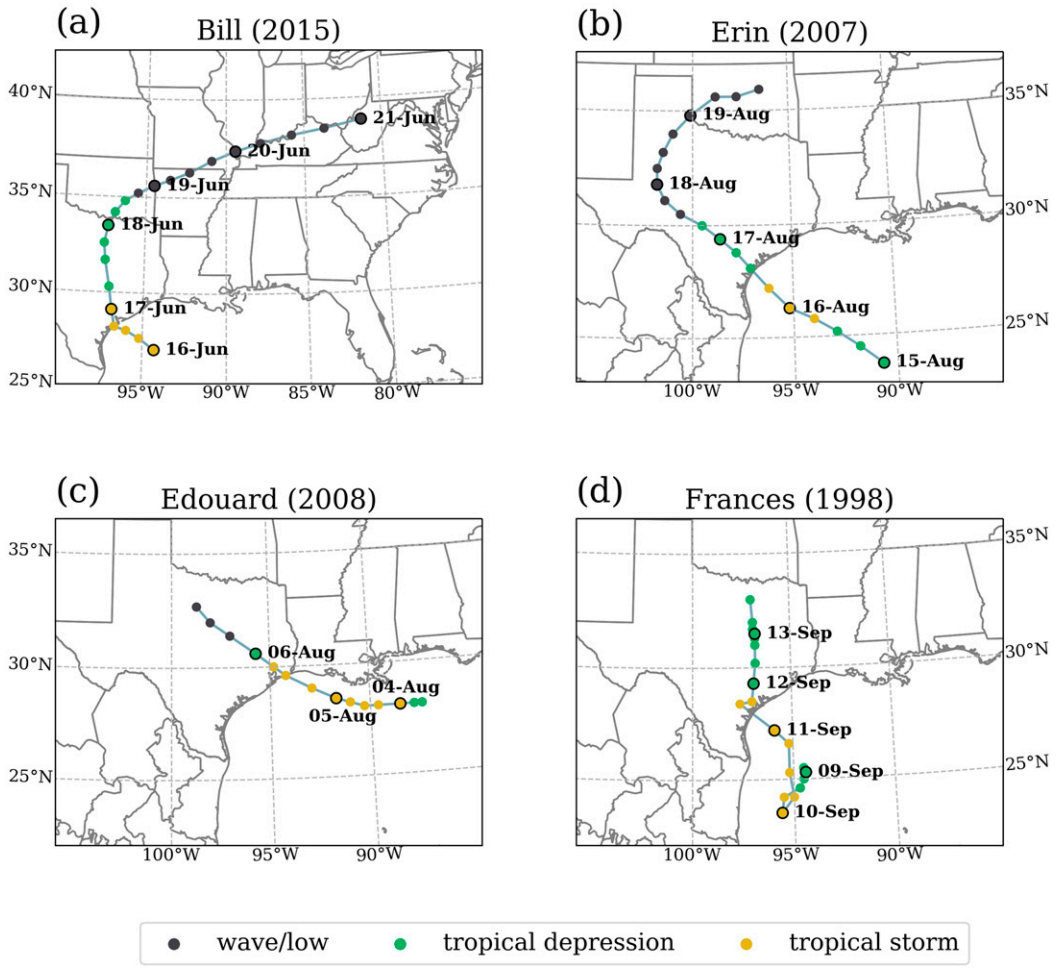

FIG. 4. NHC best track estimates for (a) Tropical Storm Bill (2015), (b) Tropical Storm Erin (2007), (c) Tropical Storm Edouard (2008), and (d) Tropical Storm Frances (1998). 0000 UTC location is given for each date, while colors correspond to intensity.

evolution by ensuring that the supply of moisture from the land surface was above average.

We also selected two tropical cyclones which weakened rapidly after landfall for analysis to identify the primary differences between TCMI and non-TCMI environments. The selected storms met the following criteria:

1) must be within the temporal coverage of the NARR dataset (1979–2019),
2) landfall occurred along the Texas coast and storm path was through northern Texas,
3) classified as a tropical storm or tropical depression at landfall,
4) weakened rapidly following landfall and did not undergo extratropical transition, and
5) overall synoptic forcing was weak.

The only two storms which met these criteria during the 1979–2018 period and were chosen for analysis were TS Frances (1998) and TS Edouard (2008). The paths of these storms are shown in Fig. 4. While the time of year for our comparison storms is later in the warm season, an already limited sample of storms made it unfeasible to obtain comparison cases which meet the above criteria and also occur as early in the season as TS Bill.

Domain averages of surface fluxes and precipitation were computed for the 2 weeks preceding the time of interest. These domains were defined by all points within a 3° radius centered upon a select point along a tropical cyclone's path. Domains for Erin and Bill were centered upon the locations along the HURDAT best track locations in which TCMI occurred, while domains during Edouard and Frances were centered upon track points that were closest to TCMI1 during TS Bill. Pressure decreases were observed from 1200 UTC 19 June to 1200 UTC 20 June for TCMI2 during TS Bill with the greatest decrease observed from 1800 UTC 19 June to 0600 UTC 20 June. Even though the location of the storm changed during this time, results showed little difference if we chose to center our domain at the earlier or later location. As such, we chose

Brought to you by UNIVERSITY OF OKLAHOMA LIBRARY | Unauthenticated | Downloaded 10/13/21 07:32 PM UTC

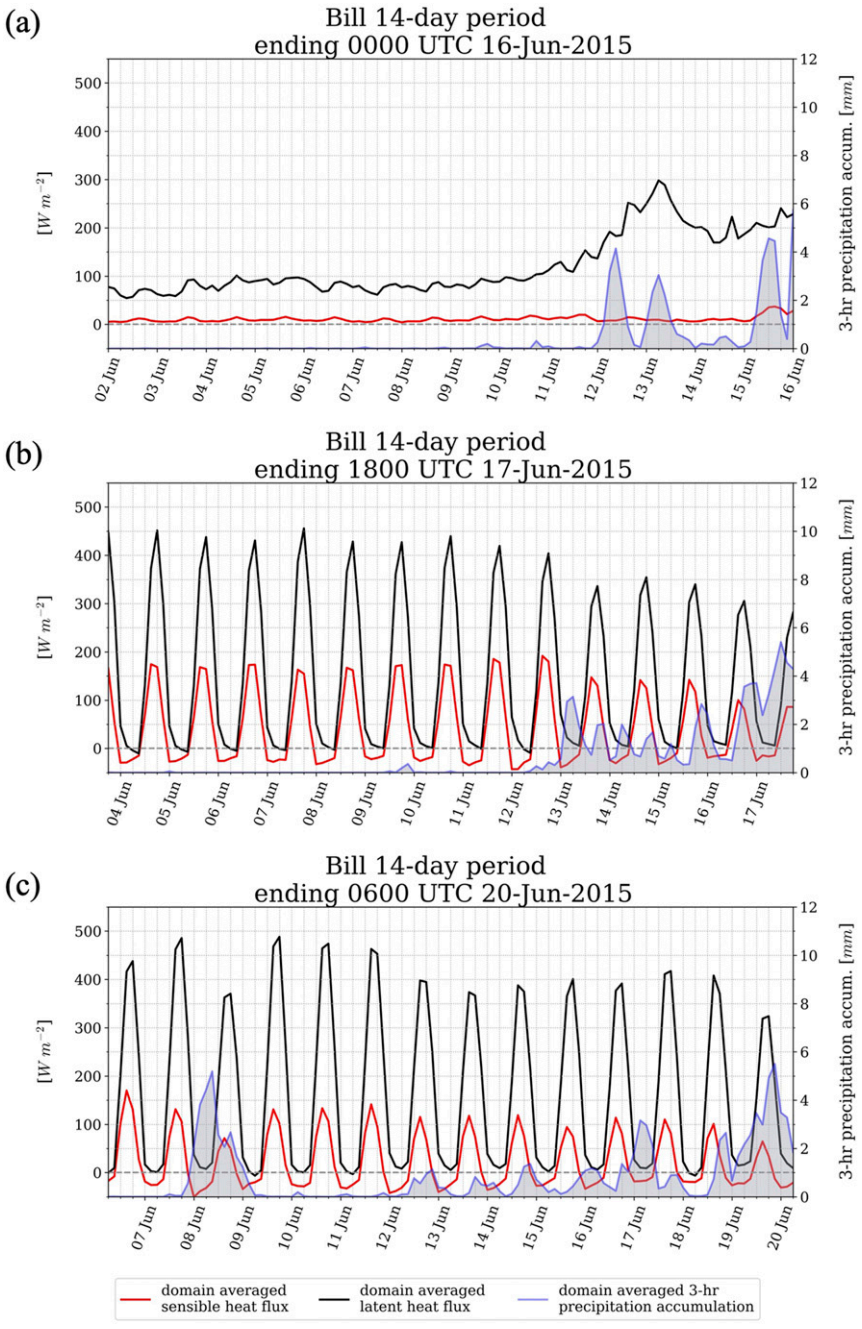

FIG. 5. Domain averaged 3-hourly latent and sensible heat fluxes and 3-hourly accumulated precipitation for the two-week period preceding (a) formation of Tropical Storm Bill, (b) TCMI1 during Tropical Storm Bill, and (c) TCMI2 during Tropical Storm Bill.

the latter as this location corresponded to approximately the same time of day as the TCMI event during Erin.

a. TCMI antecedent environments

Maximum latent heat fluxes over land for both of Bill's TCMI domains were consistently greater than maximum latent heat fluxes over the oceanic domain for the 2-week antecedent period. During the 4 days prior to Bill's formation over the ocean, maximum latent heat fluxes became more similar in magnitude to those over land and were 200–300 W m^{-2} (Fig. 5). A main difference between oceanic (domain centered upon points along the storm's path over the ocean, Fig. 5a) and overland domains (Figs. 5b,c) is that a clear diurnal cycle exists in these fluxes over the land surface that is not observed over the ocean. Consequently, the daily average latent heat fluxes over the land surface during the antecedent 2-week period for

Brought to you by UNIVERSITY OF OKLAHOMA LIBRARY | Unauthenticated | Downloaded 10/13/21 07:32 PM UTC

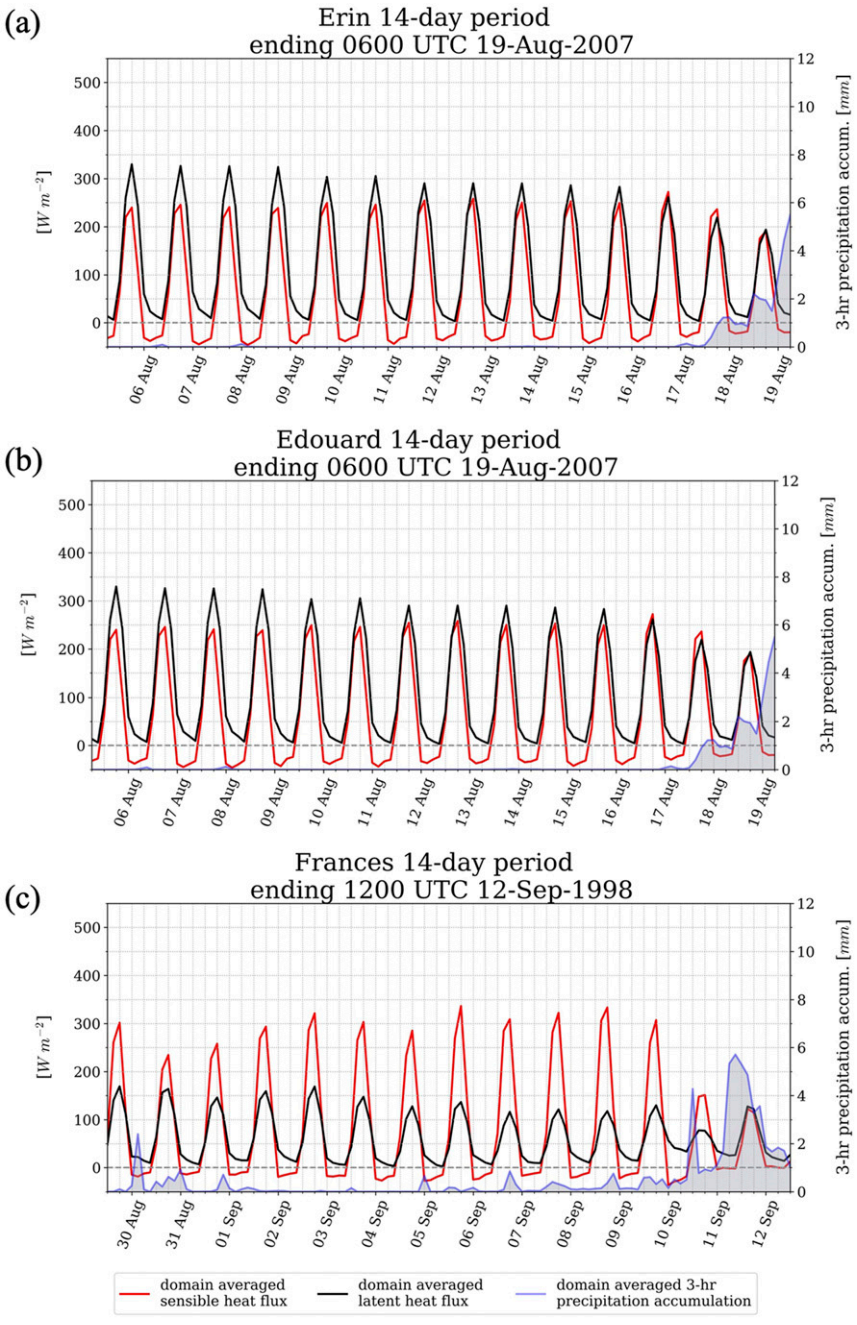

FIG. 6. As in Fig. 5, but for (a) TCMI during Tropical Storm Erin, (b) non-TCMI during Edouard, and (c) non-TCMI during Frances.

each TCMI domain were approximately 150 W m^{-2}, which was comparable to the daily average latent heat fluxes over the ocean (approximately 125 W m^{2}) for the same length of time.

Both TCMI domains during Bill also displayed multiple days with precipitation during the antecedent period, allowing for maintenance of terrestrial moisture which then supported ample latent heat fluxes. Sensible heat fluxes over both oceanic and TCMI domains were considerably smaller than latent heat fluxes.

We compared pre-TCMI environments during Bill to that of TS Erin (Fig. 6a), given 1) numerous studies (Arndt et al. 2009; Kellner et al. 2012; Andersen and Shepherd 2013; Andersen et al. 2013) have already shown that TS Erin's reintensification over land was likely tied to anomalous latent heat fluxes, and 2) we would expect pre-TCMI environments during TS Erin and TS Bill to share similar characteristics. In fact, daily maximum latent heat fluxes prior to TS Bill were greater than before Erin, while sensible heat fluxes were comparatively lower than

Brought to you by UNIVERSITY OF OKLAHOMA LIBRARY | Unauthenticated | Downloaded 10/13/21 07:32 PM UTC

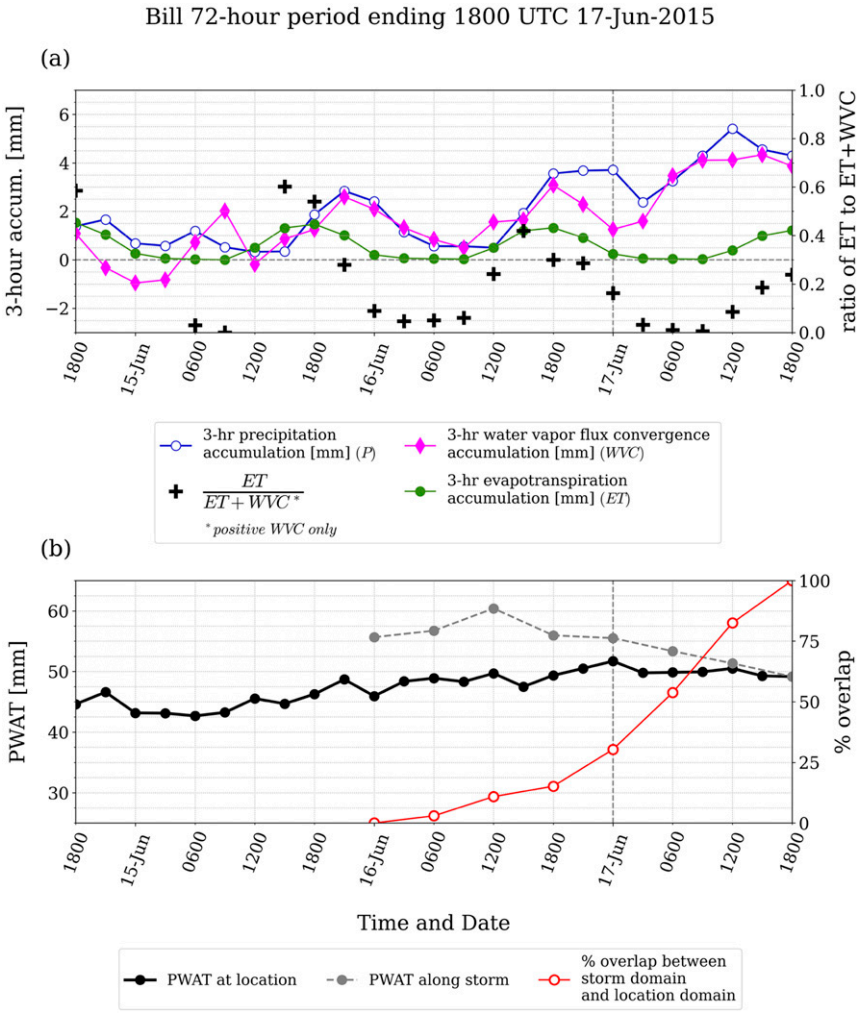

FIG. 7. Water vapor budget during the 72-h period preceding TCMI1 with (a) domain averaged, 3-hourly accumulated precipitation (mm; blue line); total column water vapor flux convergence (WVC; mm; magenta line), evapotranspiration (ET; mm; green line); and ratio of ET to sum of ET and WVC (dimensionless; crosses). Ratio was only computed when WVC is positive. (b) Temporal variation in PWAT (mm) within domain of interest (solid black line), temporal variation along path of TS Bill (dashed teal line), and percent overlap between moving domain centered along storm's path and the current domain (solid red line).

before Erin. Andersen et al. (2013) showed that sensible heat fluxes prior to Erin were greater than sensible heat flux magnitudes observed for three other TCMI events which did not occur in North America. We found that latent and sensible heat flux magnitudes prior to TS Bill were similar to the other three pre-TCMI environments they analyzed.

b. *Non-TCMI antecedent environments*

The magnitudes of *sensible* heat fluxes over the land surface prior to Edouard were nearly identical to the magnitudes of *latent* heat fluxes during Bill. Daily averaged latent heat fluxes during the two weeks preceding TS Edouard (Fig. 6b) and TS Frances (Fig. 6c) were less than 40 W m^{-2} while daily averaged sensible heat fluxes were 132 and 90 W m^{2}, respectively.

Rainfall in the 48 h preceding Frances was associated with a reduction in sensible heat fluxes such that they became similar in magnitude to latent heat fluxes. This precipitation was likely associated with cloud cover from the approaching TC, which reduced net radiation, and therefore reduced the magnitude of sensible and latent heat fluxes. This will be discussed further in the next two sections.

6. 72-h antecedent environment water vapor budget

Soil moisture memory can reflect antecedent precipitation anomalies which occurred several weeks to several months prior, and this memory manifests itself in the partitioning of surface fluxes (Entin et al. 2000; Basara and Crawford 2002; Wu and Dickinson 2004). However, the impact of these fluxes

Brought to you by UNIVERSITY OF OKLAHOMA LIBRARY | Unauthenticated | Downloaded 10/13/21 07:32 PM UTC

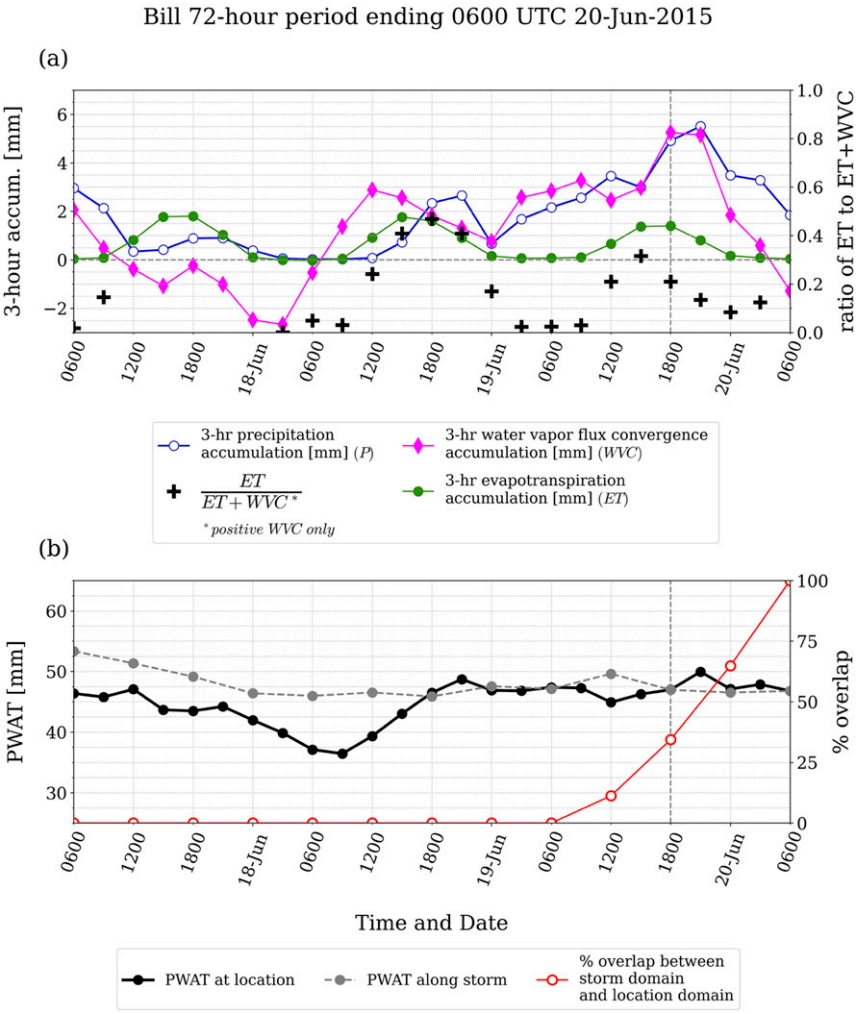

FIG. 8. As in Fig. 7, but for the 72-h period preceding TCMI2.

on atmospheric moisture content is still constrained by the typical residence time of moisture in the atmosphere. The average residence time of moisture in the atmosphere over the Great Plains can vary seasonally but is usually on the order of 3–5 days (Läderach and Sodemann 2016). Therefore, we also investigated the atmospheric moisture budget over a 3-day antecedent time window for each domain.

We primarily focused on domain averages of the three components of the atmospheric moisture budget—precipitation, ET, and WVC—and their impacts on the total column PWAT. Domain averages were computed over all points within a 0.5° radius of the storm center, as described in section 4. ET was defined as a 3-h accumulation at each 3-h time step and can be obtained from

$$\mathrm{ET} = \frac{\overline{\mathrm{LHF}} \times \Delta t}{\rho L_v}, \tag{1}$$

where Δt is given in seconds, $\overline{\mathrm{LHF}}$ is the 3-hourly latent heat flux obtained from the NARR, ρ is the density of water, and L_v is the latent heat of vaporization.

Precipitation contributes negatively to PWAT tendency, while WVC can have positive or negative contributions and ET generally has a positive contribution except at night over land. Therefore, ET can provide a compensating source of moisture when WVC is negative and may serve as an additional source when it is positive. Figures 7 and 8 show that precipitation and water vapor flux convergence increased prior to each TCMI event during Bill, while ET displayed a diurnal cycle. To better understand the relative *positive* contribution of ET to the water vapor budget, we computed the ratio of ET to the sum of ET and WVC only when WVC was positive (Figs. 7a and 8a). During daytime hours, this ratio was often >0.2. In other words, ET had about 20% of all positive contributions to the atmospheric moisture budget.

Finally, we consider whether much of the moisture budget terms considered are driven by the tropical cyclone circulation itself, rather than the precursor environment. PWAT was averaged over all points within a 3° radius, stationary domain, corresponding to the storm's location at the time of interest. For example, PWAT was computed during the preceding 72-h within a domain corresponding to TS Bill's center during TCMI1,

Brought to you by UNIVERSITY OF OKLAHOMA LIBRARY | Unauthenticated | Downloaded 10/13/21 07:32 PM UTC

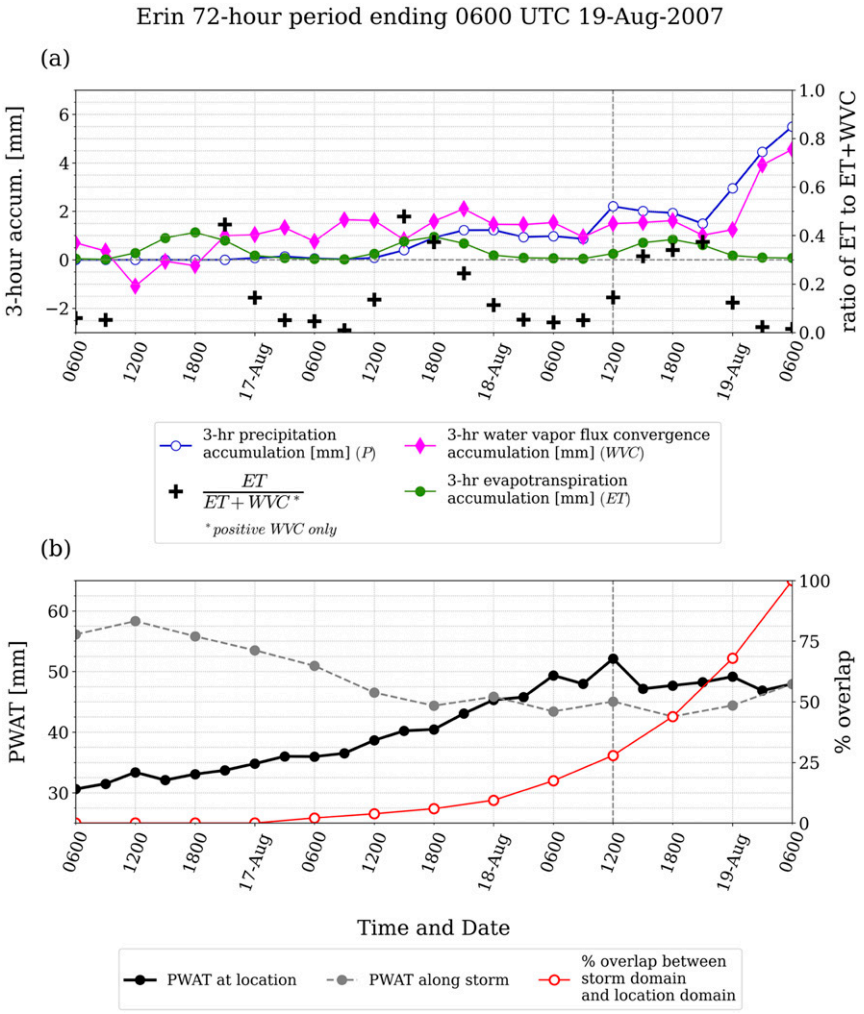

FIG. 9. As in Fig. 7, but for the 72-h period preceding TCMI during Erin.

or 1800 UTC 17 June (Fig. 7). We also computed a moving domain of the same size as the stationary domains which were also defined by a 3° radius *along* the path of the tropical cyclone to determine when the TCMI domain began to overlap significantly with the stationary tropical cyclone domain. Figures 7b–11b show the temporal evolution of PWAT along the path of the tropical cyclone as well as the temporal evolution of PWAT within the stationary domain. Comparing these two values allowed us to determine the magnitude of the difference between PWAT within the circulation and the environment that it was moving toward. A larger difference would support weakening of the cyclone, while smaller differences would aid in maintenance. From 15 to 17 June, <30% of the domain overlapped with the tropical cyclone, while both WVC and ET provided positive contributions to the atmospheric water vapor budget, and PWAT slightly increased (Fig. 7). Furthermore, we showed that WVC and precipitation alone were not sufficient to estimate the actual PWAT tendency during this time; however, without considering ET, the actual tendency of PWAT was underestimated suggesting that ET played a nonnegligible role in the atmospheric moisture budget prior to TCMI1.

During the daytime hours of 18 June, prior to TCMI2, PWAT increased over the domain to about the same as the along-TC domain, though the two domains did not overlap (Fig. 8c). WVC contributed most to PWAT tendency during this time; however, without considering ET, the actual tendency of PWAT was underestimated (Fig. 8b).

Similar results were observed prior to TCMI during Erin (Fig. 9), where ET was often at least half of the magnitude of WVC, and ignoring ET once again underestimated PWAT tendency. Conversely, during Edouard and Frances, including ET provided little impact to the estimation of PWAT tendency, while WVC and precipitation played a dominant role in the tendency of PWAT within each domain.

While both Frances (Fig. 10) and Edouard (Fig. 11) had smaller magnitudes of ET than Erin and Bill, they also had smaller magnitudes of WVC as the tropical cyclone approached each domain, despite close proximity to the Gulf of Mexico. The TCMI1 domain during Bill was also within a

Brought to you by UNIVERSITY OF OKLAHOMA LIBRARY | Unauthenticated | Downloaded 10/13/21 07:32 PM UTC

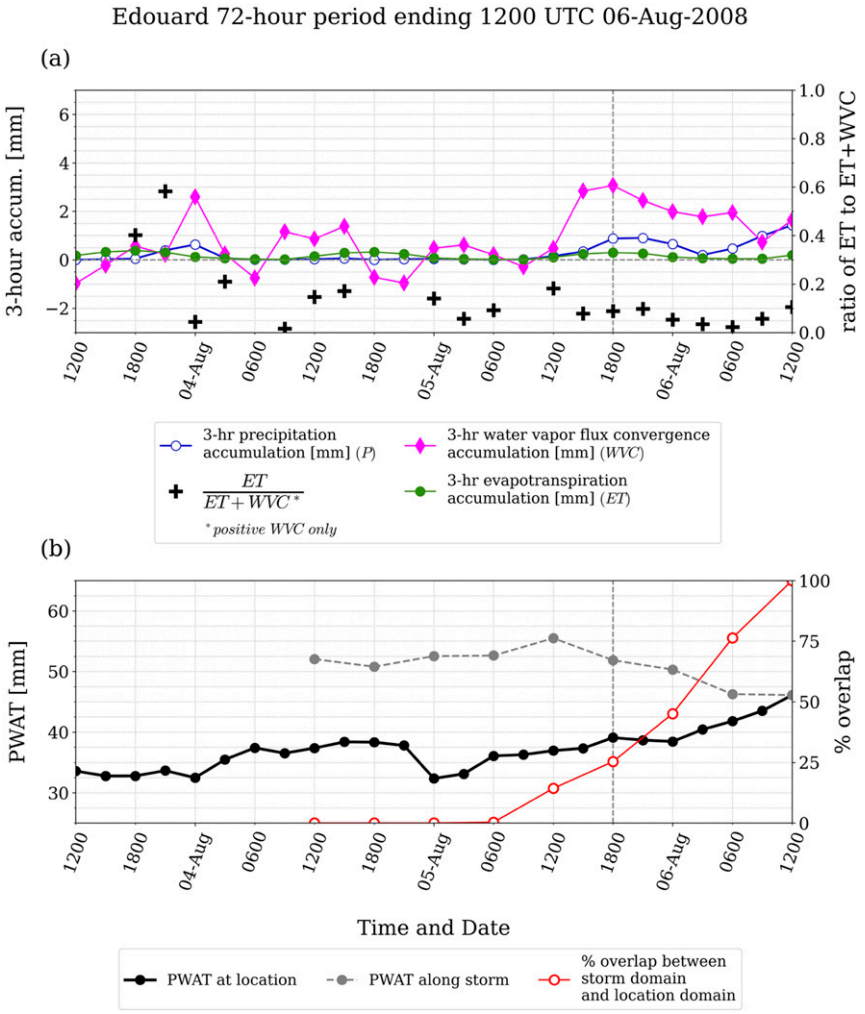

FIG. 10. As in Fig. 7, but for the 72-h period preceding 1200 UTC 6 Aug 2008 during Tropical Storm Edouard.

similar location to Frances and Edouard but was characterized by greater WVC. Even TCMI2 during Bill and TCMI during Erin, with domains much further from oceanic moisture sources, still displayed larger WVC than that observed prior to Edouard and Frances. We hypothesize that latent heat fluxes from a moist land surface along TC inflow may have influenced the maintenance of TS Bill over land, especially during TCMI2. Such upstream influences have, in fact, been shown to occur over the ocean, where inflow parcels can gain moisture from the underlying sea surface and support tropical cyclone development (Fujiwara et al. 2017). In other words, positive WVC during TCMI events during TS Bill and TS Erin may not be independent of influences from upstream latent heat fluxes.

7. 24-h backward trajectory analysis

We use backward trajectories to determine the relative path of inflow parcels for each domain considered, and the nature of latent heat fluxes along these paths. The origin of air parcels within the inflow and the lower troposphere surrounding the TC was identified using the Hybrid Single-Particle Lagrangian Integrated Trajectory (HYSPLIT) model (Stein et al. 2015). HYSPLIT-generated backward trajectories were computed using 3D temperature, moisture and wind fields from NARR. Past applications of the HYSPLIT model are extensive and include the identification of moisture sources during extreme precipitation events (Gustafsson et al. 2010; Bracken et al. 2015; Jana et al. 2018), and identification of TC parcel moisture source regions (Fritz and Wang 2013; Wang et al. 2018), including for TS Erin (Monteverdi and Edwards 2010). Therefore, the application of the HYSPLIT model to current analyses is well justified. The objective of this analysis is to understand the potential influence of land ET within boundary layers along the path of each parcel.

Parcel backward trajectories were released from eight horizontal planes at heights of 0, 100, 250, 500, 750, 1000, 1500, and 2000 m AGL. Each horizontal plane contained 169 release points (Fig. 12) distributed within a 3° × 3° grid at 0.5° intervals,

Brought to you by UNIVERSITY OF OKLAHOMA LIBRARY | Unauthenticated | Downloaded 10/13/21 07:32 PM UTC

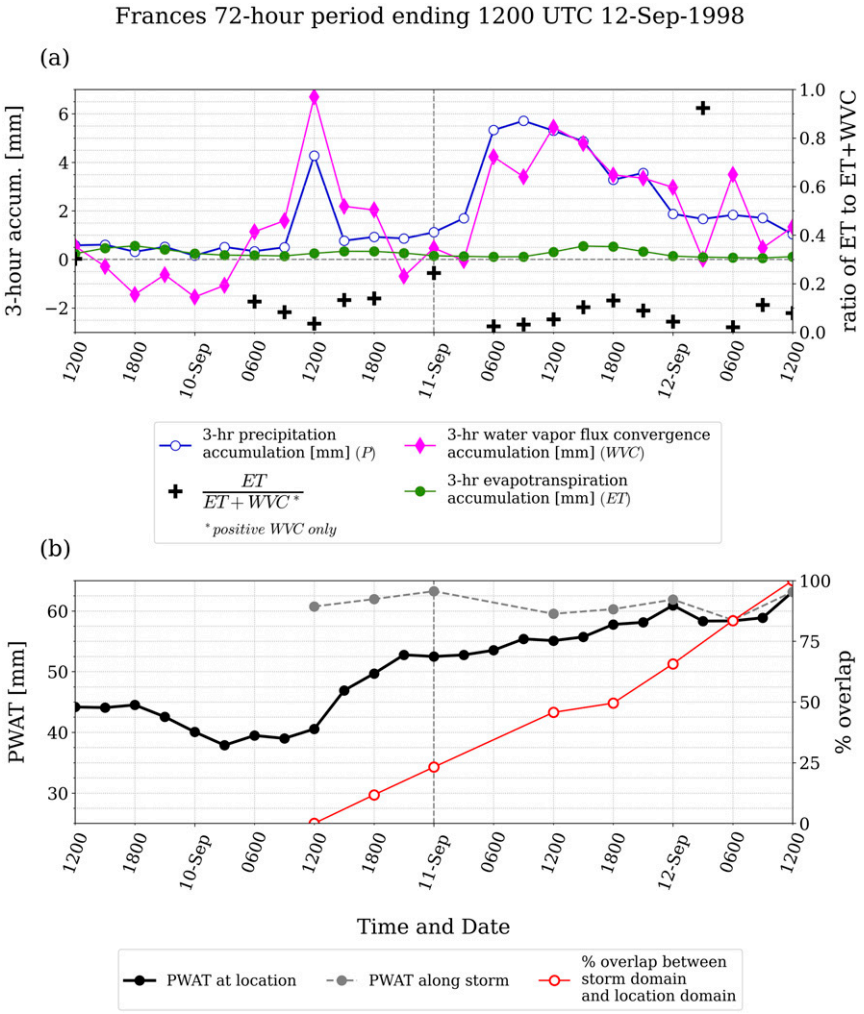

FIG. 11. As in Fig. 7, but for the 72-h period preceding 1200 UTC 13 Sep 1998 during Tropical Storm Frances.

and these planes were centered upon the domains analyzed in the previous sections. Parcels were released and traced backward in time for the preceding 24-h period. For example, one trajectory release plane was centered upon the HURDAT latitude and longitude of TS Bill's center at 0600 UTC 20 June, and trajectories from this location were traced backward from this time to 0600 19 June. In most cases, low-level TC inflow is maximized below 1000 m (Zhang et al. 2013), thus the choice of vertical levels was primarily focused on representing the inflow layer.

Parcels within the planetary boundary layer (PBL) were binned to the nearest NARR grid box to determine the relative spatial distribution of all instances along every trajectory in which a parcel was within the PBL. One major assumption of this method is that parcels within a well-mixed PBL can be influenced by surface fluxes of moisture and can represent surface influence on parcel moisture uptake or loss (Erlingis et al. 2019a,b). This assumption may be especially limited in the vicinity of a TC. However, it does provide a first guess as to where land/oceanic surface fluxes may be influential along TC inflow. Backward trajectories also provide a slightly different definition of precursor environment, with information about the origin of parcels entering the TC inflow region. Finally, we computed the accumulated evapotranspiration for every NARR grid box corresponding to a point within the PBL along one more trajectories during the 24-h periods in which backward trajectories were analyzed.

a. *ET along TCMI inflow trajectories*

Accumulated ET in the 24-h period preceding TCMI1, not surprisingly, was maximized over the Gulf of Mexico with values $> 10\,\text{mm day}^{-1}$ (Fig. 13a). Some of the storm's circulation was still over the Gulf of Mexico at the start of the antecedent 24-h period, such that wind speeds at tropical storm intensity would have encouraged elevated latent heat fluxes over water. Over land, accumulated evapotranspiration was

Brought to you by UNIVERSITY OF OKLAHOMA LIBRARY | Unauthenticated | Downloaded 10/13/21 07:32 PM UTC

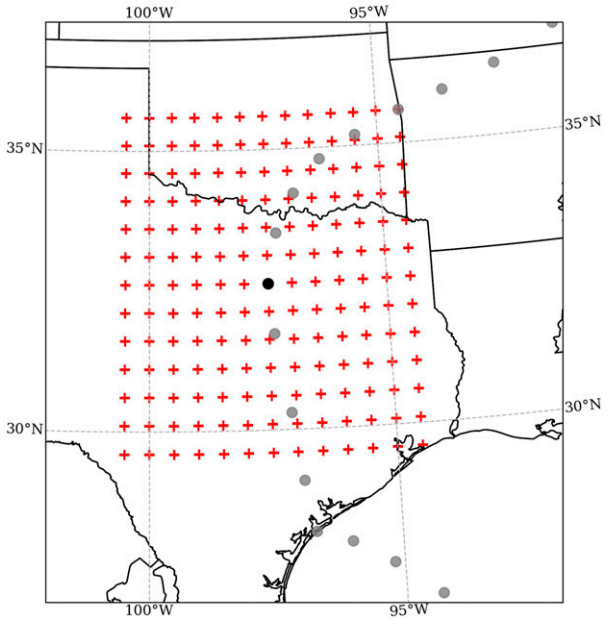

FIG. 12. Example horizontal trajectory release grid for 1800 UTC 17 Jun 2015 for a single level. Red crosses represent trajectory release points, and the black marker represents the location of TS Bill at the time of interest while gray markers represent the path of TS Bill.

considerably smaller than over the ocean, but still considerable, especially when compared to non-TCMI cases (Fig. 14). During Bill's TCMI1, both accumulated continental ET (Fig. 13a) and parcel frequency (Fig. 13b) were locally maximized to the right of the TC track and in particular along the Texas and Louisiana border where ET was approximately 5 mm day^{-1}.

Similarly, maximum ET values of 5–7 mm day^{-1} were observed along the path of inflow parcels during the 24-h period preceding TCMI2 (Figs. 13c,d). The greatest number of boundary layer inflow parcels was concentrated over Alabama, central Tennessee, and Kentucky, where ET was also maximized during this time. More importantly, boundary layer parcels during this 24-h period had origins that were almost exclusively over land. As such, not only had the TC itself resided over land for over 36 h, but most parcels within its inflow were also subjected to influence of the land surface for at least 24 h.

During TS Erin (Fig. 13e,f), ET values exceeding 5 mm day^{-1} were not as widespread over land as they were during TS Bill, but ET again was maximized locally where parcel frequencies were also maximized from eastern Oklahoma through eastern Texas. Accumulated ET over land along parcel paths for both TS Bill and TS Erin was maximized between 5 and 7 mm day^{-1}.

b. ET along non-TCMI inflow trajectories

Accumulated ET magnitudes over land during TS Edouard (Figs. 14a,b) and during TS Frances (Figs. 14c,d) were drastically smaller than those observed during TS Bill and TS Erin. Trajectory frequency plots indicate that some inflow parcels during Edouard and Frances still had oceanic origins, though the greatest concentration of parcels in both cases was still over land. The greatest concentration of PBL parcels during TS Frances occurred in northeastern Texas where accumulated ET was minimized.

The mechanisms limiting ET during Frances were different from those during Edouard, as Frances was stationary over the domain during the antecedent 24-h period. ET in this region is sensitive to changes in soil moisture and/or atmospheric demand (Guo et al. 2006; Koster et al. 2011; Wei et al. 2016). Even if outer rainbands moistened the land surface in the region adjacent to the storm, persistent cloud cover over the same region limited surface fluxes of heat and moisture. In this case, latent heat fluxes along trajectories were limited by available energy or atmospheric demand. Latent heat fluxes over land are subjected to a diurnal cycle and thus sensitive to the amount of incoming solar radiation. Over open water latent heat fluxes are more consistent during the day and at night and are sensitive to other factors such as wind speed. Over land, cloud cover associated with the TC reduces downward net radiation during the day and subsequently reduces ET (Tuleya 1994). Thus, when TS Frances became stationary over land, and most inflow parcels were also concentrated over land, the storm effectively cut itself off from land surface sources of moisture both locally and upstream via reduced net radiation. Conversely, the continued movement of TS Bill and TS Erin may have also been beneficial to sustaining intensity over land by ensuring cloud cover was not as persistent along parcel paths. Even though Edouard, like Erin and Bill, was not stationary, latent heat fluxes in the prestorm environment and along parcel inflow were driven more by a lack of surface-based moisture. Latent heat fluxes were limited over Edouard's domain during the antecedent 2-week period, suggesting limited soil moisture that was not recharged by the minimal precipitation accumulation observed during the same period.

Finally, we examined whether the observed differences in accumulated ET prior to TCMI versus non-TCMI storms were statistically significant through comparison of composite ET distributions. We computed the cumulative relative frequency of parcels within defined accumulated ET bins for non-TCMI storms and TCMI storms separately to create relative cumulative distribution functions based upon accumulated ET. The non-TCMI distribution was created from binning accumulated ET for both TS Edouard and TS Frances, while the TCMI distribution was created from binning accumulated ET for both TS Bill and TS Erin. Cumulative distribution functions were obtained for parcel trajectories and accumulated ET only for the 24-h periods ending at the times shown in Fig. 14. Domains were defined as any point along backward trajectories when parcels were within the boundary layer. Accumulated ET in each NARR grid box was weighted by the number of parcel counts in the composite backward trajectory analyses. These distributions are shown in Fig. 15. More than half of TCMI inflow parcels were within the boundary layer over regions where accumulated ET exceeded 4 mm day^{-1}, while less than 10% of non-TCMI parcels

Brought to you by UNIVERSITY OF OKLAHOMA LIBRARY | Unauthenticated | Downloaded 10/13/21 07:32 PM UTC

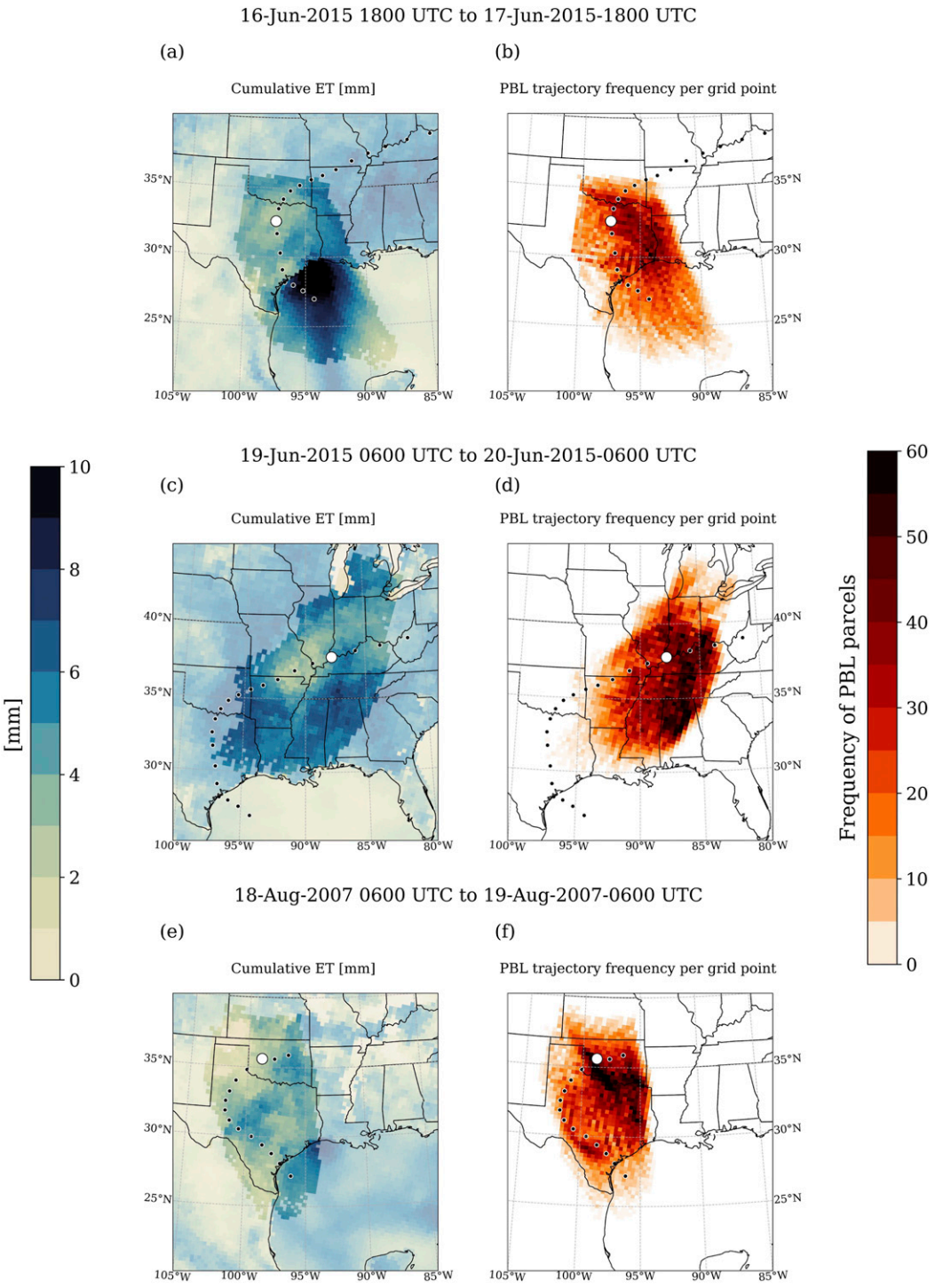

FIG. 13. (left) 24-h accumulated ET and (right) frequency of parcels along inflow trajectories that were within the boundary layer for the 24-h period preceding (a),(b) TCMI1 during Tropical Storm Bill; (c),(d) TCMI2 during Tropical Storm Bill; and (e),(f) TCMI during Tropical Storm Erin.

encountered the same environment. The two distributions are significantly different from each other ($p < 0.05$) per a two-sample Kolmogorov–Smirnov test following Wilks (2011). A major limitation of this analysis is that our sample size is limited by geography and by TCMI occurrence; therefore, we show that these *particular* TCMI and non-TCMI events are different. Future work could benefit from including TCMI and non-TCMI cases that are not

Brought to you by UNIVERSITY OF OKLAHOMA LIBRARY | Unauthenticated | Downloaded 10/13/21 07:32 PM UTC

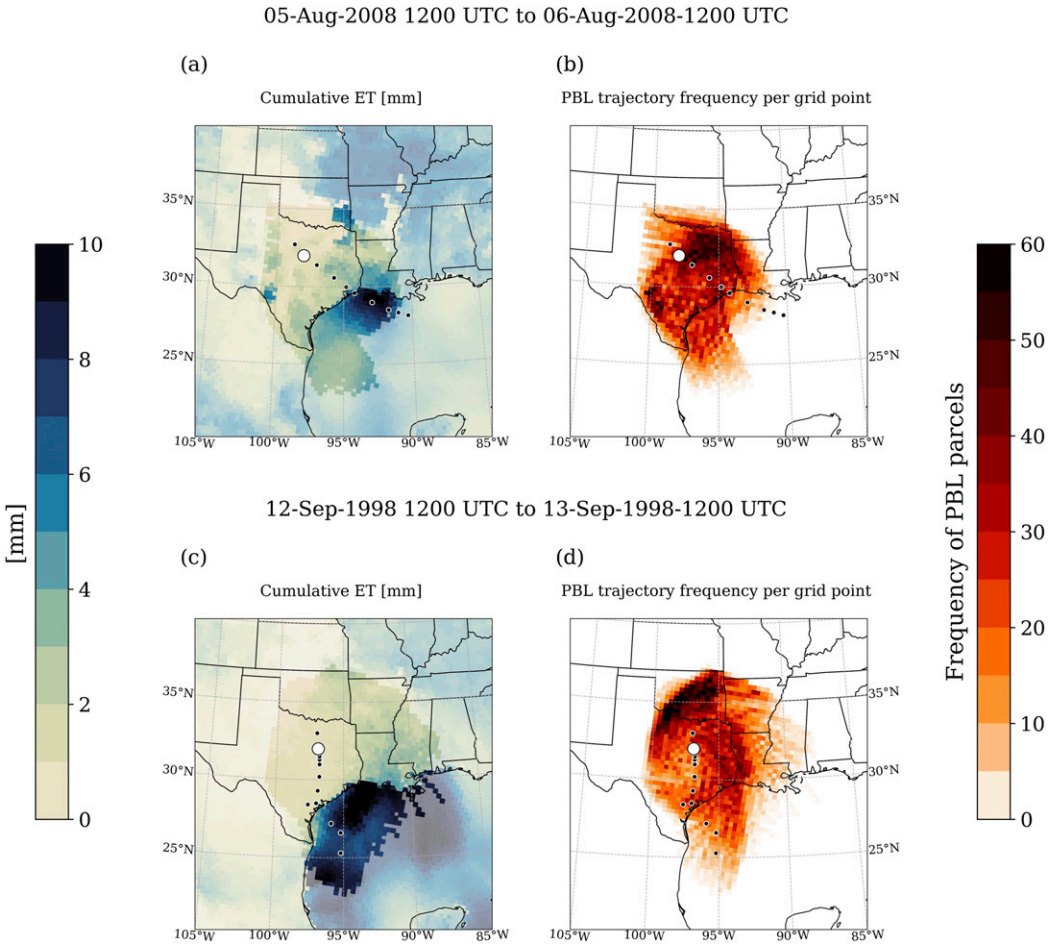

FIG. 14. As in Fig. 12, but for (a),(b) 24-h period preceding 1200 UTC 06 Aug 2008 during Edouard and (c),(d) 24-h period preceding 1200 UTC 13 Sep 1998 during Frances.

subject to the geographic limitations outlined in our data and methods.

8. Summary and conclusions

Notable differences in the antecedent environment were observed for non-TCMI and TCMI storms analyzed in this study. The 2-week antecedent periods for TCMI storms were characterized by larger latent heat flux magnitudes than sensible heat flux magnitudes with daily maxima in latent heat fluxes exceeding 200 W m^{-2} which is consistent with previous analyses of TCMI storms. Antecedent environments 2 weeks prior to non-TCMI storms were characterized by much greater sensible than latent heat flux magnitudes.

Analysis of the water vapor budget 3 days prior to each storm indicated that approximations of PWAT tendency prior to TCMI storms were underestimated when only WVC and precipitation were considered. Positive contributions from ET during daytime hours were of sufficient magnitude that inclusion of ET in the approximated PWAT tendency provided an estimation that was more similar to reality. The opposite was true for the water vapor budget prior to non-TCMI storms. PWAT tendency approximations were not sensitive to inclusion of ET as ET magnitudes were much smaller than those observed preceding TCMI storms. In both TCMI and non-TCMI cases WVC appeared to have the greatest positive contributions to the water vapor budget.

While WVC played a primary role in the water vapor budget, Fujiwara et al. (2017) showed that latent heat fluxes from the ocean can moisten inflow parcels along a moist conveyor belt and contribute to further strengthening of a tropical cyclone. As such, we considered that even large-scale moisture transport into each storm in the current analysis may have been impacted by latent heat fluxes along parcel paths. Using 24-h backward trajectories, we showed that daily accumulated ET along the path of inflow parcels was greater for TCMI storms than for non-TCMI storms. This was particularly true when only parcels over land were considered as the difference in distributions of accumulated ET along inflow parcels over land for non-TCMI and TCMI storms was statistically significant ($p < 0.05$).

Thus, we demonstrate that TCMI and non-TCMI storms displayed distinct differences in latent heat flux (or ET) within

Brought to you by UNIVERSITY OF OKLAHOMA LIBRARY | Unauthenticated | Downloaded 10/13/21 07:32 PM UTC

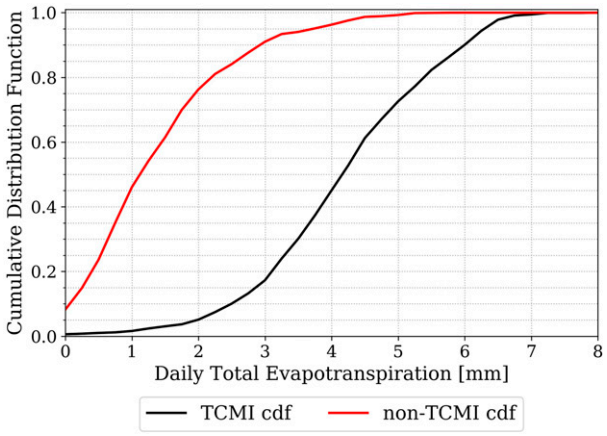

FIG. 15. Cumulative distribution function for all boundary layer parcels binned by 24-h accumulated ET (mm) for TCMI and non-TCMI storms.

the antecedent environment and along storm inflow. Interestingly, the mechanisms by which latent heat flux is reduced along parcel inflow and in the antecedent environment seem to be less important. For example, both Edouard and Frances displayed much smaller latent heat fluxes in the 2-week antecedent environment than were observed prior to Bill and Erin. Both non-TCMI environments were dominated by sensible heat fluxes 2 weeks prior to the storm. Small flux magnitudes during the 72-h period preceding Frances were likely driven by limited net radiation as the storm was nearly stationary over the domain from 12 June through 13 June. Conversely, minimal latent heat fluxes preceding Edouard were accompanied by large sensible heat fluxes implying sufficient net radiation and a drier land surface that limited evapotranspiration rather than limited evapotranspiration driven by cloud cover from the storm itself. Nevertheless, both storms were characterized by limited ET from the land surface and decayed rapidly following landfall.

The results presented offer a new approach for characterizing the prestorm environment in the analysis of overland tropical cyclones. While we followed traditional approaches of characterizing fluxes over the domain the storm would eventually occupy, we also considered whether storm inflow could be impacted by the underlying land surface. Our sample size was limited, and the primary objective was to determine whether TS Bill exhibited characteristics of TCMI during its multiday trek over land. To accomplish this task, we compared observation-based reanalysis data during TS Bill to TS Erin as it made landfall in a similar location and shared some early path overlap with TS Bill. We also applied the new trajectory-based approach to TS Erin to determine whether the two storms shared similarities in this definition of prestorm environment, and we made comparisons to non-TCMI storms, TS Edouard (2008) and TS Frances (1998) that made landfall in similar locations and followed similar post-landfall paths to TS Bill.

We show that TS Bill exhibited multiple characteristics of a TCMI storm, including its maintenance of tropical characteristics over land (Part II). Furthermore, the prestorm environment was characterized by substantial contributions to the water vapor budget from evapotranspiration and was similar to other pre-TCMI environments in the literature (Andersen and Shepherd 2013). TCMI and non-TCMI storms displayed statistically significant differences in accumulated evapotranspiration along parcel inflow suggesting that for inland tropical cyclones, evapotranspiration along inflow parcels may also play a role in their maintenance and/or reintensification. The objective of this study is not to question the existence of the brown ocean effect, but rather to determine whether TS Bill exhibited similar characteristics to other landfalling tropical cyclones which maintained intensity or underwent reintensification over land. We present evidence that TS Bill's prestorm environment supported its maintenance over land and provide a new approach for characterizing and defining the prestorm environment via inflow parcel trajectories. Using this new approach, we demonstrated a statistically significant ($p < 0.05$) difference in ET along parcel inflow trajectories for TCMI versus non-TCMI storms. Our geographic restrictions limited our sample size and future observational and reanalysis-based work should include analysis of potential TCMI and non-TCMI storms which made landfall at points beyond the Texas and Louisiana Gulf coasts. Zhang et al. (2018) showed that excessive precipitation during Hurricane Harvey may have been related not to latent heat fluxes, but rather, to enhanced surface roughness over the urban region. We attempted to account for differences in land surface characteristics by selecting storms with similar paths, such that they would be subjected to similar surface roughness, and soil texture. Even so, these variables can still vary over small distances. Other land surface characteristics not analyzed in this study, like vegetation and albedo, can vary from year to year. As such, future work should include model simulations of TS Bill to determine the storm's sensitivity to not only latent heat fluxes, but to surface roughness, albedo, soil texture, and other land surface characteristics, as well as variations due to storm intensity; however, that is beyond the scope of the current analysis.

Acknowledgments. This work was supported by the Future Investigators in NASA Earth Space Science and Technology (FINESST) Award 80NSSC19K1365 and National Science Foundation Grant Awards ICER1663840 and OIA-1946093. We would also like to acknowledge Dr. David Considine and generous support from the NASA MAP Program Grant 80NSSC17K0264. NCEP Reanalysis data provided by the NOAA/OAR/ESRL PSL, Boulder, Colorado, from their website at https://psl.noaa.gov/. The authors would also like to thank the reviewers for their comments and suggestions on this manuscript, which ultimately improved the quality and presentation of our study.

Data availability statement. NCEP North American Regional Reanalysis data used in this study was provided by the NOAA/OAR/ESRL PSL, Boulder, Colorado, and can be accessed at https://psl.noaa.gov/data/gridded/data.narr.html. National Hurricane Center Best Track data (HURDAT2) that were used in this study can be accessed at https://www.nhc.noaa.gov/data/#hurdat.

Brought to you by UNIVERSITY OF OKLAHOMA LIBRARY | Unauthenticated | Downloaded 10/13/21 07:32 PM UTC

REFERENCES

Andersen, T. K., and J. M. Shepherd, 2013: A global spatiotemporal analysis of inland tropical cyclone maintenance or intensification. *Int. J. Climatol.*, **34**, 391–402, https://doi.org/10.1002/joc.3693.

——, D. E. Radcliffe, and J. M. Shepherd, 2013: Quantifying surface energy fluxes in the vicinity of inland-tracking tropical cyclones. *J. Appl. Meteor. Climatol.*, **52**, 2797–2808, https://doi.org/10.1175/JAMC-D-13-035.1.

Arndt, D. S., J. B. Basara, R. A. McPherson, B. G. Illston, G. D. Mcmanus, and D. B. Demko, 2009: Observations of the overland reintensification of Tropical Storm Erin (2007). *Bull. Amer. Meteor. Soc.*, **90**, 1079–1094, https://doi.org/10.1175/2009BAMS2644.1.

Basara, J. B., and K. C. Crawford, 2002: Linear relationships between root-zone soil moisture and atmospheric processes in the planetary boundary layer. *J. Geophys.*, **107**, 4274, https://doi.org/10.1029/2001JD000633.

Berg, R., 2015: National Hurricane Center tropical cyclone report: Tropical Storm Bill (AL022015). NOAA, 31 pp., https://www.nhc.noaa.gov/data/tcr/AL022015_Bill.pdf.

Bozeman, M. L., D. Niyogi, S. Gopalakrishnan, F. D. Marks, X. Zhang, and V. Tallapragada, 2011: An HWRF-based ensemble assessment of the land surface feedback on the post-landfall intensification of Tropical Storm Fay (2008). *Nat. Hazards*, **63**, 1543–1571, https://doi.org/10.1007/s11069-011-9841-5.

Bracken, C., B. Rajagopalan, M. Alexander, and S. Gangopadhyay, 2015: Spatial variability of seasonal extreme precipitation in the western United States. *J. Geophys. Res.: Atmos.*, **120**, 4522–4533, https://doi.org/10.1002/2015JD023205.

Branch, O., and V. Wulfmeyer, 2019: Deliberate enhancement of rainfall using desert plantations. *Proc. Natl. Acad. Sci. USA*, **116**, 18 841–18 847, https://doi.org/10.1073/pnas.1904754116.

Brauer, N. S., J. B. Basara, P. E. Kirstetter, R. A. Wakefield, C. R. Homeyer, J. Yoo, J. M. Shepherd, and J. A. Santanello Jr., 2021: The inland maintenance and reintensification of Tropical Storm Bill (2015). Part II: Precipitation microphysics. *J. Hydrometeor.*, **22**, 2695–2711, https://doi.org/10.1175/JHM-D-20-0151.1.

Chang, H.-I., D. Niyogi, A. Kumar, C. M. Kishtawal, J. Dudhia, F. Chen, U. C. Mohanty, and M. Shepherd, 2009: Possible relation between land surface feedback and the post-landfall structure of monsoon depressions. *Geophys. Res. Lett.*, **36**, L15826, https://doi.org/10.1029/2009GL037781.

Dastoor, A., and T. N. Krishnamurti, 1991: The landfall and structure of a tropical cyclone, The sensitivity of model predictions to soil moisture parameterizations. *Bound.-Layer Meteor.*, **55**, 345–380, https://doi.org/10.1007/BF00119809.

Dirmeyer, P. A., 2006: The hydrologic feedback pathway for land-climate coupling. *J. Hydrometeor.*, **7**, 857–867, https://doi.org/10.1175/JHM526.1.

Edwards, R., 2010: Tropical cyclone tornado records for the modernized National Weather Service era. *25th Conf. on Severe Local Storms*, Denver, CO, Amer. Meteor. Soc., P2.7, https://ams.confex.com/ams/25SLS/techprogram/paper_175269.htm.

Emanuel, K. A., C. DesAutels, C. Holloway, and R. Korty, 2004: Environmental control of tropical cyclone intensity. *J. Atmos. Sci.*, **61**, 843–858, https://doi.org/10.1175/1520-0469(2004)061<0843:ECOTCI>2.0.CO;2.

——, J. Callaghan, and P. Otto, 2008: A hypothesis for the redevelopment of warm-core cyclones over northern Australia. *Mon. Wea. Rev.*, **136**, 3863–3872, https://doi.org/10.1175/2008MWR2409.1.

Entin, J. K., A. Robock, K. Y. Vinnikov, S. E. Hollinger, S. Liu, and A. Namkhai, 2000: Temporal and spatial scales of observed soil moisture variations in the extratropics. *J. Geophys. Res.*, **105**, 11 865–11 877, https://doi.org/10.1029/2000JD900051.

Erlingis, J. M., J. J. Gourley, and J. B. Basara, 2019a: Diagnosing moisture sources for flash floods in the United States. Part I: Kinematic trajectories. *J. Hydrometeor.*, **20**, 1495–1509, https://doi.org/10.1175/JHM-D-18-0119.1.

——, ——, and ——, 2019b: Diagnosing moisture sources for flash floods in the United States. Part II: Terrestrial and oceanic sources of moisture. *J. Hydrometeor.*, **20**, 1511–1531, https://doi.org/10.1175/JHM-D-18-0120.1.

Evans, C., R. S. Schumacher, and T. J. Galarneau, 2011: Sensitivity in the overland reintensification of Tropical Cyclone Erin (2007) to near-surface soil moisture characteristics. *Mon. Wea. Rev.*, **139**, 3848–3870, https://doi.org/10.1175/2011MWR3593.1.

Findell, K. L., and E. A. B. Eltahir, 2003: Atmospheric controls on soil moisture–boundary layer interactions. Part I: Framework development. *J. Hydrometeor.*, **4**, 552–569, https://doi.org/10.1175/1525-7541(2003)004<0552:ACOSML>2.0.CO;2.

Ford, T. W., A. D. Rapp, and S. M. Quiring, 2015: Does afternoon precipitation occur preferentially over dry or wet soils in Oklahoma? *J. Hydrometeor.*, **16**, 874–888, https://doi.org/10.1175/JHM-D-14-0005.1.

Frank, W. M., 1977: The structure and energetics of the tropical cyclone I. Storm structure. *Mon. Wea. Rev.*, **105**, 1119–1135, https://doi.org/10.1175/1520-0493(1977)105<1119:TSAEOT>2.0.CO;2.

Fritz, C., and Z. Wang, 2013: A numerical study of the impacts of dry air on tropical cyclone formation: A development case and a nondevelopment case. *J. Atmos. Sci.*, **70**, 91–111, https://doi.org/10.1175/JAS-D-12-018.1.

Fujiwara, K., R. Kawamura, H. Hirata, T. Kawano, M. Kato, and T. Shinoda, 2017: A positive feedback process between tropical cyclone intensity and the moisture conveyor belt assessed with Lagrangian diagnostics. *J. Geophys. Res. Atmos.*, **122**, 12 502–12 521, https://doi.org/10.1002/2017JD027557.

Guillod, B. P., B. Orlowsky, D. G. Miralles, A. J. Teuling, and S. I. Seneviratne, 2015: Reconciling spatial and temporal soil moisture effects on afternoon rainfall. *Nat. Commun.*, **6**, 6443, https://doi.org/10.1038/ncomms7443.

Guo, Z., and Coauthors, 2006: GLACE: The Global Land–Atmosphere Coupling Experiment. Part II: Analysis. *J. Hydrometeor.*, **7**, 611–625, https://doi.org/10.1175/JHM511.1.

Gustafsson, M., D. Rayner, and D. Chen, 2010: Extreme rainfall events in southern Sweden: Where does the moisture come from? *Tellus*, **62A**, 605–616, https://doi.org/10.1111/j.1600-0870.2010.00456.x.

Hart, R. E., and J. L. Evans, 2001: A climatology of the extratropical transition of Atlantic tropical cyclones. *J. Climate*, **14**, 546–564, https://doi.org/10.1175/1520-0442(2001)014<0546:ACOTET>2.0.CO;2.

Jana, S., B. Rajagopalan, M. A. Alexander, and A. J. Ray, 2018: Understanding the dominant sources and tracks of moisture for summer rainfall in the southwest United States. *J. Geophys. Res. Atmos.*, **123**, 4850–4870, https://doi.org/10.1029/2017JD027652.

Jones, S. C., and Coauthors, 2003: The extratropical transition of tropical cyclones: Forecast challenges, current understanding, and future directions. *Wea. Forecasting*, **18**, 1052–1092, https://doi.org/10.1175/1520-0434(2003)018<1052:TETOTC>2.0.CO;2.

Kellner, O., D. Niyogi, M. Lei, and A. Kumar, 2012: The role of anomalous soil moisture on the inland reintensification of Tropical Storm Erin (2007). *Nat. Hazards*, **63**, 1573–1600, https://doi.org/10.1007/s11069-011-9966-6.

Kishtawal, C. M., D. Niyogi, A. Kumar, M. L. Bozeman, and O. Kellner, 2011: Sensitivity of inland decay of North Atlantic tropical cyclones to soil parameters. *Nat. Hazards*, **63**, 1527–1542, https://doi.org/10.1007/s11069-011-0015-2.

Brought to you by UNIVERSITY OF OKLAHOMA LIBRARY | Unauthenticated | Downloaded 10/13/21 07:32 PM UTC

——, ——, B. Rajagopalan, M. Rajeevan, N. Jaiswal, and U. C. Mohanty, 2013: Enhancement of inland penetration of monsoon depressions in the Bay of Bengal due to prestorm ground wetness. *Water Resour. Res.*, **49**, 3589–3600, https://doi.org/10.1002/wrcr.20301.

Koster, R. D., and M. J. Suarez, 2001: Soil moisture memory in climate models. *J. Hydrometeor.*, **2**, 558–570, https://doi.org/10.1175/1525-7541(2001)002<0558:SMMICM>2.0.CO;2.

——, and Coauthors, 2004: Regions of strong coupling between soil moisture and precipitation. *Science*, **305**, 1138–1140, https://doi.org/10.1126/science.1100217.

——, and Coauthors, 2006: GLACE: The Global Land-Atmosphere Coupling Experiment. Part I: Overview. *J. Hydrometeor.*, **7**, 590–610, https://doi.org/10.1175/JHM510.1.

——, and Coauthors, 2011: The second phase of the Global Land–Atmosphere Coupling Experiment: Soil moisture contributions to subseasonal forecast skill. *J. Hydrometeor.*, **12**, 805–822, https://doi.org/10.1175/2011JHM1365.1.

Läderach, A., and H. Sodemann, 2016: A revised picture of the atmospheric moisture residence time. *Geophys. Res. Lett.*, **43**, 924–933, https://doi.org/10.1002/2015GL067449.

Landsea, C. W., and J. L. Franklin, 2013: Atlantic hurricane database uncertainty and presentation of a new database format. *Mon. Wea. Rev.*, **141**, 3576–3592, https://doi.org/10.1175/MWR-D-12-00254.1.

Mesinger, F., and Coauthors, 2006: North American Regional Reanalysis. *Bull. Amer. Meteor. Soc.*, **87**, 343–360, https://doi.org/10.1175/BAMS-87-3-343.

Monteverdi, J. P., and R. Edwards, 2010: The redevelopment of a warm core structure in Erin: A case of inland tropical storm formation. *Electron. J. Severe Storms Meteor.*, **5**, 1–18.

Nair, U. S., and Coauthors, 2019: Influence of land cover and soil moisture based brown ocean effect on an extreme rainfall event from a Louisiana Gulf Coast tropical system. *Sci. Rep.*, **9**, 17136, https://doi.org/10.1038/s41598-019-53031-6.

Namias, J., 1988: The 1988 summer drought over the Great Plains: A classic example of air-sea-land interaction. *Trans. Amer. Geophys. Union*, **69**, 1067.

Niyogi, D., C. Kishtawal, S. Tripathi, and R. S. Govindaraju, 2010: Observational evidence that agricultural intensification and land use change may be reducing the Indian summer monsoon rainfall. *Water Resour. Res.*, **46**, W03533, https://doi.org/10.1029/2008WR007082.

Rubin-Oster, B., 2015: Tropical Depression Bill advisory number 18. Weather Prediction Center, https://www.wpc.ncep.noaa.gov/tropical/tropical_advisories.php?storm=BILL&adnum=18&dt=2015062009&status=td.

Santanello, J. A., J. Roundy, and P. A. Dirmeyer, 2015: Quantifying the land–atmosphere coupling behavior in modern reanalysis products over the U.S. Southern Great Plains. *J. Climate*, **28**, 5813–5829, https://doi.org/10.1175/JCLI-D-14-00680.1.

Shen, W., I. Ginis, and R. E. Tuleya, 2002: A numerical investigation of land surface water on landfalling hurricanes. *J. Atmos. Sci.*, **59**, 789–802, https://doi.org/10.1175/1520-0469(2002)059<0789:ANIOLS>2.0.CO;2.

Stein, A. F., R. R. Draxler, G. D. Rolph, B. J. B. Stunder, M. D. Cohen, and F. Ngan, 2015: NOAA's HYSPLIT atmospheric transport and dispersion modeling system. *Bull. Amer. Meteor. Soc.*, **96**, 2059–2077, https://doi.org/10.1175/BAMS-D-14-00110.1.

Stewart, S. R., 2016: National Hurricane Center annual summary: 2015 Atlantic hurricane season. NHC Tech. Rep., 16 pp., https://www.nhc.noaa.gov/data/tcr/summary_atlc_2015.pdf.

Tawfik, A. B., and P. A. Dirmeyer, 2014: A process-based framework for quantifying the atmospheric preconditioning of surface-triggered convection. *Geophys. Res. Lett.*, **41**, 173–178, https://doi.org/10.1002/2013GL057984.

Taylor, C. M., R. A. M. de Jeu, F. Guichard, P. P. Harris, and W. A. Dorigo, 2012: Afternoon rain more likely over drier soils. *Nature*, **489**, 423–426, https://doi.org/10.1038/nature11377.

Tuleya, R. E., 1994: Tropical storm development and decay: Sensitivity to surface boundary conditions. *Mon. Wea. Rev.*, **122**, 291–304, https://doi.org/10.1175/1520-0493(1994)122<0291:TSDADS>2.0.CO;2.

——, and Y. Kurihara, 1978: A numerical simulation of the landfall of tropical cyclones. *J. Atmos. Sci.*, **35**, 242–257, https://doi.org/10.1175/1520-0469(1978)035<0242:ANSOTL>2.0.CO;2.

Wang, Y., Y. Huang, and X. Cui, 2018: Impact of mid- and upper-level dry air on tropical cyclone genesis and intensification: A modeling study of Durian (2001). *Adv. Atmos. Sci.*, **35**, 1505–1521, https://doi.org/10.1007/s00376-018-8039-0.

Wei, J., H. Su, and Z.-L. Yang, 2016: Impact of moisture flux convergence and soil moisture on precipitation: A case study for the southern United States with implications for the globe. *Climate Dyn.*, **46**, 467–481, https://doi.org/10.1007/s00382-015-2593-2.

Wilks, D. S., 2011: *Statistical Methods in the Atmospheric Sciences*. 3rd ed. Elsevier, 676 pp.

Wu, J., and P. A. Dirmeyer, 2020: Drought demise attribution over CONUS. *J. Geophys. Res. Atmos.*, **125**, e2019JD031255, https://doi.org/10.1029/2019JD031255.

Wu, W., and R. E. Dickinson, 2004: Time scales of layered soil moisture memory in the context of land–atmosphere interaction. *J. Climate*, **17**, 2752–2764, https://doi.org/10.1175/1520-0442(2004)017<2752:TSOLSM>2.0.CO;2.

Yosef, G., R. Walko, R. Avisar, F. Tatarinov, E. Rotenberg, and D. Yakir, 2018: Large-scale semi-arid afforestation can enhance precipitation and carbon sequestration potential. *Sci. Rep.*, **8**, 996, https://doi.org/10.1038/s41598-018-19265-6.

Zhang, F., Z. Pu, and C. Wang, 2019: Impacts of soil moisture on the numerical simulation of a post-landfall storm. *J. Meteor. Res.*, **33**, 206–218, https://doi.org/10.1007/s13351-019-8002-8.

——, ——, and ——, 2020: Land-surface diurnal effects on the asymmetric structures of a postlandfall tropical storm. *J. Geophys. Res. Atmos.*, **126**, e2020JD033842, https://doi.org/10.1029/2020JD033842.

Zhang, J. A., R. F. Rogers, P. D. Reasor, E. W. Uhlhorn, and F. D. Marks, 2013: Asymmetric hurricane boundary layer structure from dropsonde composites in relation to the environmental vertical wind shear. *Mon. Wea. Rev.*, **141**, 3968–3984, https://doi.org/10.1175/MWR-D-12-00335.1.

Zhang, W., G. Villarini, G. A. Vecchi, and J. A. Smith, 2018: Urbanization exacerbated the rainfall and flooding caused by Hurricane Harvey in Houston. *Nature*, **563**, 384–388, https://doi.org/10.1038/s41586-018-0676-z.

Brought to you by UNIVERSITY OF OKLAHOMA LIBRARY | Unauthenticated | Downloaded 10/13/21 07:32 PM UTC